LAWRENCE
LIVERMORE
NATIONAL
LABORATORY

LLNL-TR-643814

# Strangeness Production in ALICE at the LHC

A. Harton, R. Carmona, M. Tyler, R. Soltz

September 12, 2013

## Disclaimer



This work performed under the auspices of the U.S. Department of Energy by Lawrence Livermore National Laboratory under Contract DE-AC52-07NA27344.

# Strangeness Production in ALICE at the LHC

Austin Harton, Rodney Carmona, Micheal Tyler, Ron Soltz and Edmundo Garcia
Chicago State University, Lawrence Livermore National Laboratory

## Introduction

At the most fundamental level, ordinary matter is composed of quarks and gluons bound together to form hadrons. The protons and neutrons that form atomic nuclei are members of this class. At most temperatures quarks are very tightly bound together by gluons, the particles which carry the strong force, however, at extremely high temperatures equal to approximately 100,000 times that at the sun's core, the quarks possess the energy to separate and transition to a state of matter consisting of individual quarks and gluons. In this state the quarks and gluons are asymptotically free [1]. This state is known as the Quark Gluon Plasma (QGP) is believed to be the state of matter a few microseconds after the Big Bang. \ Over the last thirty years several laboratories have been focused on creating the (QGP) in a controlled environment so that its properties can be more easily investigated. Programs at the "Relativistic Heavy Ion Collider (RHIC)" at Brookhaven National Laboratory (BNL) and more recently the Large Hadron Collider (LHC)'s "A Large Ion Collider Experiment (ALICE)" at the European Center for Nuclear Research (CERN) have been dedicated to exploring the physics of the QGP. In heavy ion collisions, experiment has shown that an indicator of the existence of the QGP is the enhancement of strange hadrons emanating from the collision [2].

In understanding the enhancement of strange particles emitted from collisions it is noted that no strange quarks existed in the colliding nuclei prior to the collision, from which it follows that strange quarks are created during the collision. Since strangeness is a conserved quantity, strange quarks are created as quark-antiquark pairs $(s\bar{s})$ by strong or electro-weak interactions. Additionally, since the mass of the $(s\bar{s})$ pair is comparable to the critical temperature for QGP formation it can be expected that strange particle enhancement will occur. Using perturbative QCD it has been shown that two primary mechanisms exist for strange quark creation. They are annihilation of light quarks, $q\bar{q} \rightarrow s\bar{s}$, and gluon fusion, $gg \rightarrow s\bar{s}$. The time associated with light quark annihilation was found to be too long when compared to the time needed to reach QGP equilibrium, thereby making the gluon fusion mechanism the dominant process for strange quark creation [3]. Figure 1 illustrates strange quark creation by gluon fusion in QGP and the formation of strange hadrons [4].

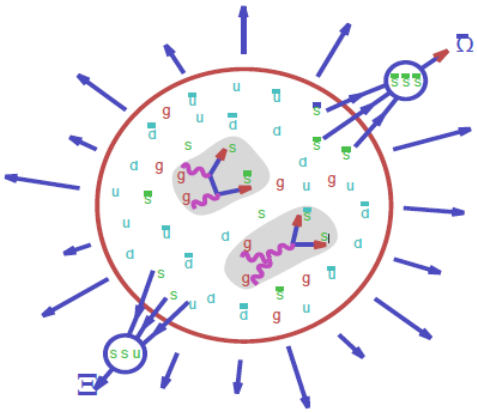

Figure 1. Illustration showing the creation of strange quarks through gluon and fusion and the formation of strange hadrons [4].

Thus the strange particles formation is highly correlated to the reaction mechanism governing the hadronic collisions. Finally, the observed strange particle yield is also sensitive to the transition from the dense state of QCD matter to a hadron gas (hadronization) where after local thermalization the entropy of the reaction is spent in the expansion or in the formation of new particles through the fragmentation (and possible recombination in non-vacuum) of quarks and gluons. The gluon fragmentation supplies the antiquarks, favoring the formation of antihyperons, further enhancing their abundance.

The abundance of gluons in the early stage of the collision leads to a rapid thermal equilibration of the strange quarks in the medium. The bulk characteristics of particles with strange or anti-strange quarks were measured at CERN by the WA97 and NA57 experiments [5,6] and more recently by the STAR experiment at RHIC [7], as shown in Fig. 2 (left). For all strange species an enhancement is observed as a function of the average number of participants $\langle N_{PART} \rangle$. The enhancement is of similar magnitude for the vastly different energy available in the reaction. Strangeness measurements at mid-$p_T$ are shown in the right panel of Fig. 2, where the $R_{CP}$ (yield per binary collision in central collisions divided by respective value in peripheral collisions) for various strange particles in $Cu+Cu$ collisions is given [7]. The mid-$p_T$ baryons have higher values compared to the strange mesons in this region. This is most likely due to coalescence providing more quarks for baryon production than mesons at the same energy. The values at higher $p_T$ appear to merge where fragmentation is expected to dominate the production.

The study of the interplay between strangeness and QCD matter can be extended to high-$p_T$ by characterizing the strangeness in jets. It is common to discuss high-energy phenomena in quantum QCD in terms of quarks and gluons. Quarks and gluons (partons) are not directly detectable. Immediately after being produced, partons are fragmented and hadronized leading to a collimated spray of energetic particles - a jet. Perturbative QCD has proven successful in

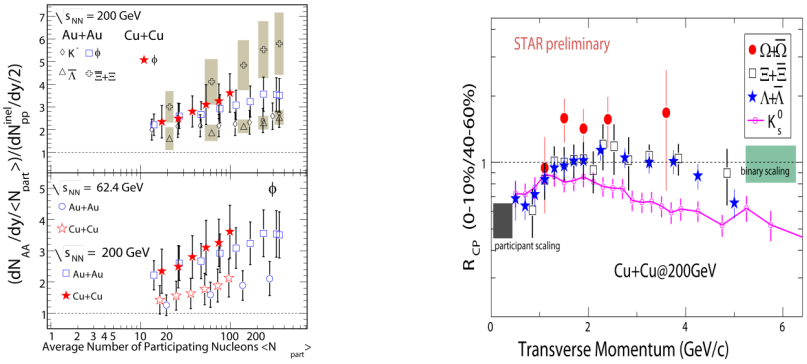


Figure 2. Left Panel: Mid-rapidity per participant yields of strange particles for Cu+Cu and Au+Au collisions normalized by the respective $p + p$ values. Right Panel: $R_{CP}$ for strange mesons and baryons in Cu+Cu $\sqrt{s}$ = 200 GeV collisions. The shaded boxes show regions where the respective scaling regimes apply.

describing inclusive hadron production in elementary collisions. Within the theory's range of applicability, calculations to next-to-leading order (NLO) produce an accurate description of charged hadron $p_T$ spectra in different collision systems and at different energies, leading to claims of universality of the underlying fragmentation functions (FF) [8]. With the *pp* data collected at RHIC and at the LHC, FF studies are now being extended to strange baryon and meson production [9,10]. The gluon-to-hadron FF are not well-constrained by $e + e^-$ and deep inelastic scattering data due to the low gluon-jet cross section. At RHIC and the LHC, it is possible to probe FF in a very gluon-jet rich environment since the majority of final states are produced by gluons. Figure 3 shows the fragmentation functions of charged hadrons, the Λ and $K^0_S$ particles for various jet energies *pp* data at √ s=200 GeV.

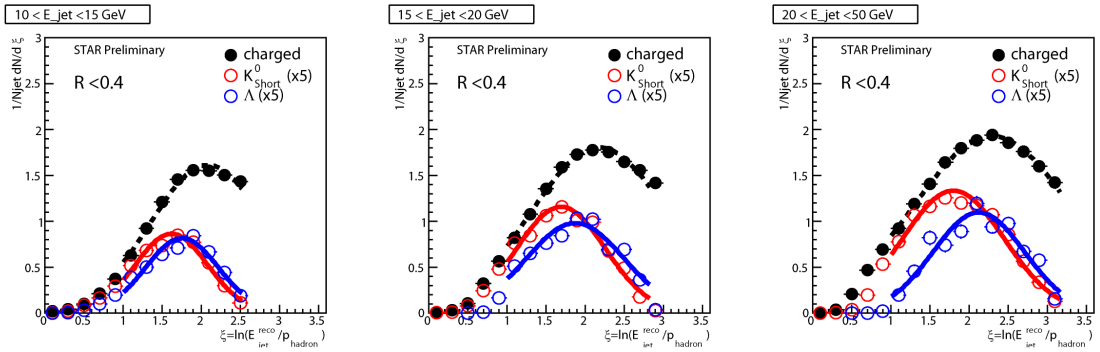


Figure 3. Fragmentation functions of charged hadrons or various jet energies. R indicates the size of jet the cone in $\Delta\eta, \Delta\phi$ space. The lines represent Gaussian fits and $\xi=\ln(Ejet/p_{Thadron})$, where $E_{jet}$ is the reconstructed jet energy.

The study of strangeness in jets would constrain the QCD-inspired jet fragmentation models, and also provides a path for understanding strangeness production in heavy-ion collision jets. For jets in elementary collisions, the hadronization prescription has been applied successfully to jet hadrochemistry: by evolving the

parton shower for different hadron species down to scales set by the hadron mass, accounting for the main characteristic differences in the hump-backed plateaus of pions, kaons and protons. If this hadronization assumption persists in the presence of a dense QCD matter, then it leads to specific predictions for the medium-modified hadrochemical composition of quenched jets [11]. Furthermore, several other dynamical mechanisms are conceivable, which may affect the hadrochemistry of jets in medium. In particular, the gluon exchange between the parton shower and the medium changes the color flow. Since hadronization must implement color neutralization, this can change significantly the hadrochemical composition of jet fragments, which can be probed by extracting flavor characteristics, specifically the strangeness of jets.

**Experimental set-up**

ALICE is a general purpose detector composed of several smaller sub-detectors built to analyze the high energy Pb-Pb, proton-proton and proton-Pb collisions. The sub-detectors are arranged inside a 0.5 T solenoid magnet. The sub-detectors have the ability to perform particle identification (PID) and fine momentum resolution over a wide momentum range. The high energy collisions of primary particles occur at the center of the ALICE detector in a vacuum beam pipe. For the work described in this document the following sub-detectors were used [12,13]:

- The Inner Tracking System (ITS) [14,15,16] is composed of six layers of silicon detectors and is innermost sub-detector in ALICE. The primary vertex (collision region) determination as well as track reconstruction is performed by the two layers that are closest to the beam pipe. These layers are comprised of Silicon Pixel Detectors (SPD). The remaining layers of the ITS are two layers made up of Silicon Drift Detectors (SDD) and the final two layers that are double sided Silicon Strip Detectors (SSD). These outer four layers are used for particle tracking and low momentum particle identification.
- The Time Projection Chamber (TPC) [17] is located in the central barrel and is the main tracking sub-detector, performing momentum measurements on charged particles emanating from the collision, particle identification and vertex determination. It is a drift detector covering a pseudo-rapidity range of $|\eta| \leq 0.9$ for tracks of full radial track length and $|\eta| \leq 1.5$ for reduced track lengths.
- The Time of Flight (TOF) [18] Detector is a cylindrical assembly used to identify charged particles in the intermediate momentum range. The TOF provides a time measurement which when used in conjunction with momentum and track length measurements provided by ALICE's tracking detectors calculates particle mass. The TOF covers a pseudo-rapidity range of $|\eta| \leq 0.9$ and full azimuth angle, except for the region where $260^0 < p < 320^0$ when $\eta$ is near zero.

- The VZERO counter [19] consists of two arrays of 32 scintillators encircling the beam pipe and on both sides of the interaction region. (VZERO-A) is located z=3.3m and covers the pseudo-rapidity range 2.8<η<5.1, and (VZERO–C ) is located at z=0.9m and covers -3.7<η<-1.7. The detector's time resolution is approximately 0.5 ns.
-

**Analysis**

As an initial phase of using strange particles as probes for the QGP, we will investigate $\Lambda$'s, $\overline{\Lambda}$'s and $K_S^0$'s, resulting from proton-proton (pp) collisions to establish a baseline for the study of strangeness in Pb-Pb collisions. Starting with pp, we will measure the strangeness yields, eventually making similar measurements in jets to understand the particle fragmentation process, setting the basis for a study in the heavy ion data. Measurements of strange particles in heavy ion collisions will provide information on the temperature of the Quark Gluon Plasma as well as the interaction of high-energy jets in the medium.

Since $\Lambda$'s, $\overline{\Lambda}$'s and $K_S^0$'s are charge neutral particles (often called $V^0$ particles) and cannot be detected as they traverse the particle detector. The only evidence of their existence is the tracks of their charged decay products which are similar to the letter "V". As a result, it is necessary to identify them by performing invariant mass analysis using the tracks of the decay products. The decay products for $\Lambda$'s, $\overline{\Lambda}$'s and $K_S^0$'s are $p\,\pi^-$, $\bar{p}\,\pi^+$, and $\pi^+\,\pi^-$, respectively. Particle identification of $V^0$ particles requires selection of daughter tracks based on their distance from the primary vertex, the distance of closest approach (DCA) and how well the momentum of the $V^0$ particle points to the primary vertex [20]. Invariant mass distributions for $K_S^0$ particles and $\Lambda$ particles were obtained and are shown in Figure 4.

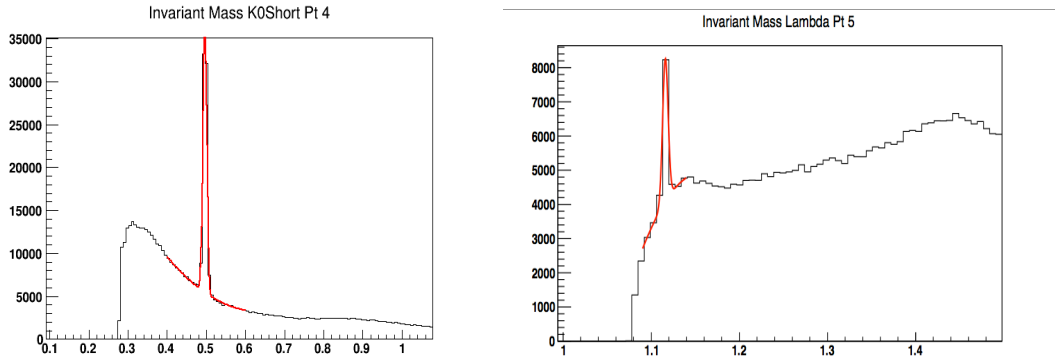


Figure 4. Invariant mass distributions for $K_S^0$ particles and $\Lambda$ particles.

In Figure 5, an Armenteros-Podolanski plot [20] is used to display the V0 candidates. In the plot $\alpha=(p_L^+ - p_L^-)/(p_L^+ + p_L^-)$ and $p_L^+$ and $p_L^-$ are the longitudinal components of the momentum of the positive and negative daughter particles

relative to the V0 particle. The $K_S^0$ particles are symmetric at $\alpha$=0 while the $\Lambda$ and $\overline{\Lambda}$ are symmetric at approximately $\alpha$=+/-0.7.

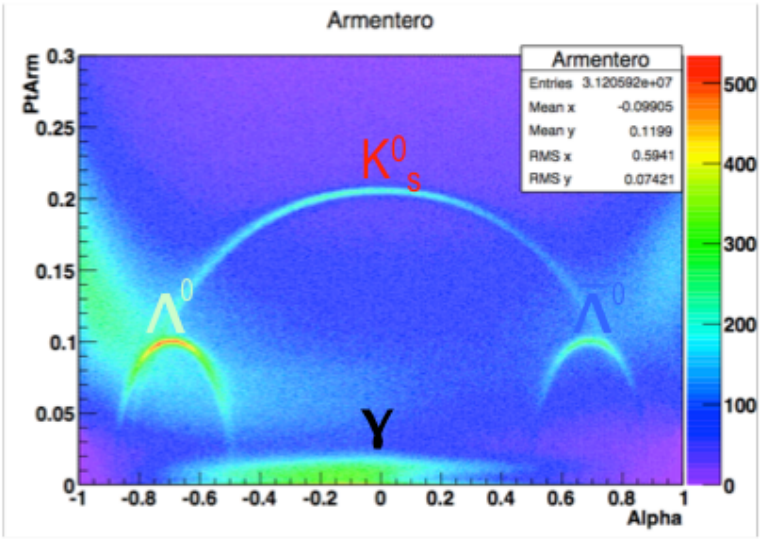

Armentero histogram

Figure 5 Armenteros-Podolanski plot where $K_S^0$, $\Lambda$ and $\overline{\Lambda}$ are clearly distinguishable among the V0 candidates.

The uncorrected spectra for $\Lambda$'s, $\overline{\Lambda}$'s and $K_S^0$'s is shown in Figure 6. The distributions of the three particles reach a peak at low $p_T$ (~1GeV/c) and then decrease at higher $p_T$.

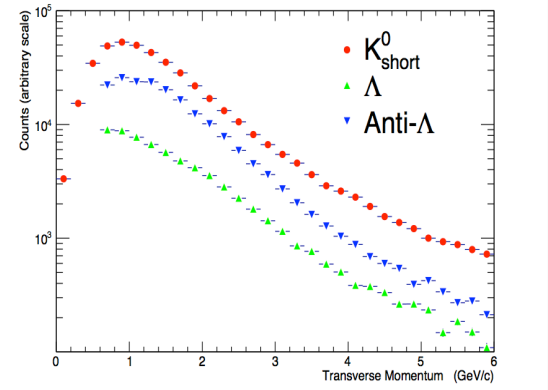


Figure 6. Particle spectra (uncorrected) as a function of $p_T$ for $\Lambda$'s, $\overline{\Lambda}$'s and $K_S^0$'s.

## Future Work

The next step in this work will be to perform efficiency correction of the data obtained using Monte Carlo techniques to propagate particles through the detector

using an event generator such as Pythia [21] and GEANT4 [22] to transport particles through the ALICE detectors [20]. The known Monte Carlo data is then propagated through the particle reconstruction and particle identification process to determine the efficiency of the reconstruction process. This efficiency is then used to correct the raw reconstruction data.
Next, we will start the analysis of data generated by Pb-Pb collisions. This will include the analysis of strange particle yields and will, also involve the investigation of strange particle jets emanating from the QGP.

## References


[1] Bohr, Henrik; Nielsen, H. B. "Hadron production from a boiling quark soup: quark model predicting particle ratios in hadronic collisions". *Nuclear Physics B* **128** (2): 275, (1977).

[2] J. Rafelski, R. Hagedorn "From Hadron Gas to Quark Matter". Statistical mechanics of quarks and hadrons, North-Holland and Elsevier. pp. 253–272. ISBN 0-444-86227-7. CERN-TH-2969 (1980).

[3] P. Koch, B. Muller and J. Rafelski,"Strangeness in relativistic heavy ion collision". Phys. Rep. 142, No. 4 (1986) 167.

[4] J. Rafelski, "Strangeness Production and Quark Gluon Plasma Properties". SQM2011, Krakow, Poland.

[5] E. Andersen *et al*. (WA97 Collaboration), "Strangeness enhancement at mid-rapidity in Pb–Pb collisions at 158 A GeV/c". Phys. Lett. B 449 (3–4): 401, 1999

[6] F. Antinori *et al*. (NA57 Collaboration). "Enhancement of hyperon production at central rapidity in 158 *A* GeV/*c* Pb+Pb collisions". Journal of Physics G **32** (4): 427, 2006

[7] A.R. Timmins *et al*. (STAR Collaboration). "Overview of strangeness production at the STAR experiment". Journal of Physics *G* **36** (6): 064006, 2009

[8] S. Albino et al., arXiv:0804.2021 [hep-ph]

[9] B. I. Abelev *et al.* [STAR Collab.], Phys. Rev. C75 (2007) 064901

[10] K. Aamodt *et al.* (ALICE Collaboration) "Strange particle production in proton–proton collisions at $\sqrt{s} = 0.9$ TeV with ALICE at the LHC" Eur. Phys. J. C 71 (3), 1594 (2011)

[11] S. Sapeta and U. A. Wiedemann, Eur. Phys. J. C **55** (2008) 293

[12] Physics Performance Report I. (ALICE Collaboration), J. Phys. G30, 1517 (2004)

[13] Physics Performance Report II. (ALICE Collaboration), J. Phys. G32, 1295 (2006)

[14] R. Santoro et. al. (ALICE Collaboration), J. Instrum. 4, P03023 (2009)

[15] P. Christakoglou et. al. (ALICE Collaboration), Proceedings of Science (EPS-HEP 2009) (2009)

[16] K. Aamodt et. al. (ALICE Collaboration), J. Instrum. 5, P03003 (2010)

[17] J. Alme, Y. Andres, H. Appelshauser, S. Bablok, N. Bialas, R. Bolgen, U. Bonnes, . Bramm, et al., Nucl. Instrum. Meth. A 622 (2010) 316

[18] A. Akindinov et. al., Eur. Phys. J. C68, 601 (2010)

[19] K. Aamodt et. al. (ALICE Collaboration), J. Instrum. 3, S08002 (2008)
[20] A. Aamodt et. al., Eur. Phys. J. C71, 1594 (2011)
[21] T. Sjostrand, S. Mrenna, P. Skands, J. High Energy Phys. 0605, 026 (2006)
[22] GEANT4 User's Guide, November 30, 2012.